Water Research 266 (2024) 122336

Contents lists available at ScienceDirect

Water Research

journal homepage: www.elsevier.com/locate/watres

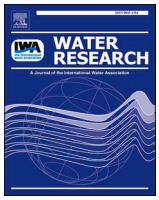

# Enrichment of dissolved metal(loid)s and microbial organic matter during transit of a historic mine drainage system

Anita Alexandra Sanchez [a,*], Karl Haas [b], Conrad Jackisch [b], Sabrina Hedrich [c], Maximilian P. Lau [a,d]

[a] Institute of Mineralogy, Technische Universität Bergakademie Freiberg, Brennhausgasse 14, 09599 Freiberg, Germany
[b] Institute of Drilling Technology and Fluid Mining, Technische Universität Bergakademie Freiberg, Germany
[c] Institute of Biosciences, Technische Universität Bergakademie Freiberg, Germany
[d] Interdisciplinary Environmental Research Centre, Technische Universität Bergakademie Freiberg, Germany

ARTICLE INFO

*Keywords:*
Mine drainage
Fluorescence
Microbial activity
Metal(loid) mobilization
Water flow
pH levels

ABSTRACT

Water quality degradation by decommissioned mining sites is an environmental issue recognized globally. In the Ore mountains of Central Europe, a wide array of contaminants is released by abandoned under- and above-ground mining sites threatening the quantity and quality of surface and groundwater resources. Here, we focus on the less-explored internal pollution processes within these mines involving organic carbon and microorganisms in trace metal(loid)s mobilization processes. Over an 18-month period, we conducted hydrological and biogeochemical monitoring at the Reiche Zeche mine, a former lead-zinc-silver mine, in Germany, reaching 230 meters below ground, well below the critical zone. Our results show strong seasonal fluctuations in water availability, concentrations of metal(loid)s, pH, and dissolved organic matter (DOM) components across multiple depths. Excess metal(loid) presence during high flow conditions indicated mobilization behavior deviating from conservative dilution. Our findings reveal strong positive correlations between metal(loid) variability and pH (0.894), and between metal(loid) variability and the DOM fluorescent component C2 (-0.910), a proxy for microbial activity. Accordingly, the microbial processes may significantly contribute to the observed metal(loid) composition and fluxes. By elucidating the intricate roles of hydrological and biogeochemical factors in trace metal(loid) mobilization, our research offers a comprehensive framework for improving mine water management and remediation, potentially informing global environmental policies and sustainable mining practices.

## 1. Introduction

Decommissioned mining infrastructure are a global phenomenon because of the mines' economic and social relevance of resource extraction during operation (Grande et al., 2018). As the number of operating mines has increased significantly over the last decades, mine abandoning will ultimately increase the number and footprint of decommissioned sites, raising health and environmental concerns (Watari et al., 2021; Tao et al., 2022). Metal(loid)s are key targets of extraction and potentially toxic elements and are regularly bound in a sulfide matrix (Root et al., 2015). Depending on the abundance of sulfide minerals in the ore e.g., in the form of pyrite ($FeS_2$), which readily oxidizes to form acidity, mine waters may be acidic or neutral, but under both conditions mine water can degrade freshwater resources and are commonly associated with serious environmental problems (Tiwary 2001, Skousen et al., 2019; Aguilar-Garrido et al., 2023). In abandoned mines without management of drainage, high levels of harmful dissolved metal(loid)s are widespread where drainage waters are acidic, whereas in non-acidic waters high total suspended solids and bacterial contaminants dominate (Tiwary 2001; Tiwary and Dhar, 1994). Release of mine drainage to surface waters is harmful for aquatic and floodplain ecosystems and can promote biodiversity loss (Kefeni et al., 2017; Dhir 2018; Aguilar-Garrido et al., 2023).

Mine drainage origins from both surface- and groundwater sources. Its subsurface flow paths control the chemical interactions with reactive materials from its points of origin to the mine drainage system and outlet (Nordstrom 2008; Wolkersdorf et al., 2022; Nascimento et al., 2023). Widely applied geochemical models (e.g., TOUGH and MIN3P) use reactive transport simulations to integrate complexation, hydrolysis, and redox reactions (Kalonji-Kabambi et al., 2020). Microorganisms

* Corresponding author.
*E-mail address:* Anita.Sanchez@mineral.tu-freiberg.de (A.A. Sanchez).

https://doi.org/10.1016/j.watres.2024.122336
Received 18 June 2024; Received in revised form 23 August 2024; Accepted 24 August 2024
Available online 28 August 2024
0043-1354/© 2024 The Author(s). Published by Elsevier Ltd. This is an open access article under the CC BY license (http://creativecommons.org/licenses/by/4.0/).

were identified as additional mediators of metal(loid) mobilization processes in mine waters (Haferburg et al., 2022; Hedrich et al., 2022) and microbial community characteristics are used as proxies for hydraulic connectivity (Merino et al, 2022). There is a need for field hydro-biogeochemical studies to fully grasp water-rock-microbe interplay and refine predictions of mine water characteristics.

From a hydrological perspective, understanding of the dynamics of a mine system and identifying dominant controls on solute concentrations is challenged by its strong spatial and temporal variability (Pohle et al., 2021; Bracken et al., 2013; Lintern et al., 2018; Reddy et al., 1999; Aguilera & Melack, 2018), despite the long integration paths of the water supply from variable and distributed sources (e.g., groundwater, rainfall, and snowmelt). In near-surface catchments, concentration-discharge (C-Q) relationships can characterize export patterns for individual runoff events and longer time series (Pohle et al., 2021; Aguilera & Melack, 2018; Hunsaker & Johnson, 2017; Bieroza & Heathwaite, 2015). The C-Q relationships help to explain the mechanisms that govern rate and extend of solute mobilization (Basu et al., 2011), and should also be applicable under the conditions of subsurface mine drainage systems.

Transport and release patterns of metal(loid)s in mine waters are shaped not only by the hydrological movement but also by the biogeochemical character of the system. Both, the release of metal(loid)s to the water phase (leaching) and the susceptibility for transport is dependent upon ambient pH, metal(loid) properties and solution speciation, including redox condition, and the presence of reactive complexation sites such as in dissolved organic matter (DOM) (Dijkstra et al., 2004). Free metal(loid) species were the dominant species below pH 4 (Durães et al., 2017), while above, metal(loid) concentration can increase with increasing amounts of DOM (Khaledian et al., 2017; Arenas-Lago et al., 2014). As described in Fest et al. (2007), high molecular size fractions in DOM promote the solubilization of heavy metals, whereas the presence of condensed organic structures appear to suppress metal mobility. Wang et al. (2023) linked DOM with microbial community composition, invoking that through the degradation of humic-like substances high amounts of labile DOM are released and support heterotrophic microorganisms in activating their iron or arsenic reducing potentials. DOM quantity and quality thus plays an important role in both abiotic and biotic process chains by altering (bio-)availability of nutrients and contaminants.

Monitoring the concentration and chemical composition of DOM has potential to elucidate the sources and fate of mine drainage waters. However, monitoring DOM quantity in mine drainage environments is challenging due to access restrictions and low concentrations (She et al., 2023). Absorbance and fluorescence spectroscopy provide valuable techniques for characterizing DOM's components, aromaticity, molecular weight, and sources (Holland et al., 2018; McKnight et al., 2001). Improved knowledge of DOM quality will aid in the ongoing exploration of the role that biogeochemical factors may play in driving metal(loid) mobilization in both acidic and neutral mine water environments (Cravotta et al., 2014; She et al., 2023).

In this study we aim to investigate the hydrological and biogeochemical controls on metal(loid)s mobilization in abandoned large-scale mining systems. The former lead-zinc-silver mine Reiche Zeche is such a system and has been converted into a research and teaching facility. In this mine, the study addresses two fundamental research questions, (1) what are the seasonal and spatial variations in water quality as drainage waters pass through the mine, and (2), how do the dynamics in mine water DOM impact the mobility and distribution of metal(loid)s in the drainage system.

Previous studies in Reiche Zeche revealed acidic waters containing high concentrations of iron, zinc, and other heavy metals when seeping through rock (Zhiteneva et al., 2016; Haferburg et al., 2022). Microbial communities in Reiche Zeche occupy biofilm-rich, acidic environments (pH $< 3.0$) within the mine (Haferburg et al., 2022). We hypothesize that significant relationships between microbial-sourced DOM, pH and metal(loid)s variability in the mine waters exist, and that they are simultaneously modified by seasonal and spatial variations. Our 18-month long sampling efforts aim to enhance our comprehension of the biogeochemical factors driving metal(loid)s mobilization, so that research at Reiche Zeche can establish a framework for addressing similar yet understudied mine systems in future research on mine water quality.

## 2. Materials and methods

### 2.1. Study site and sample collection

Located in the Ore Mountains in central Europe, the Reiche Zeche mine (50.9283° N, 13.3574° E) is one of the numerous historic mining sites that drains untreated to Elbe river tributaries (Zhiteneva et al., 2016). The operation of mining high grade minerals and mine waste rock at Reiche Zeche continued until 1969, after which the lower part of the 1300-meter-deep mine system was flooded (Zhiteneva et al., 2016). The upper 230 meters of the mine system remained above the central adit, exposing several abandoned shafts and refilled former ore seams to weathering and drainage.

For this study we focus on one slanted vertical extraction structure ("Schwarzer Hirsch Stehender") which extends over the three levels before it reaches the central drainage adit (Fig. 1): Level 1 ('Stollensohle', 103 meters below surface), 2 ('1. Sohle', 149 meters below surface), and 3 ('1/2 3. Sohle', 191 meters below surface). Along these access tunnels we identified 26 sample sites for continuous water sampling which we visited in 33 sample campaigns in three-week intervals from February 2nd, 2022 to August 3rd, 2023. 14 out of the 26 sample sites had high flowing waters, providing a larger proportion of the drainage than the drip sites.

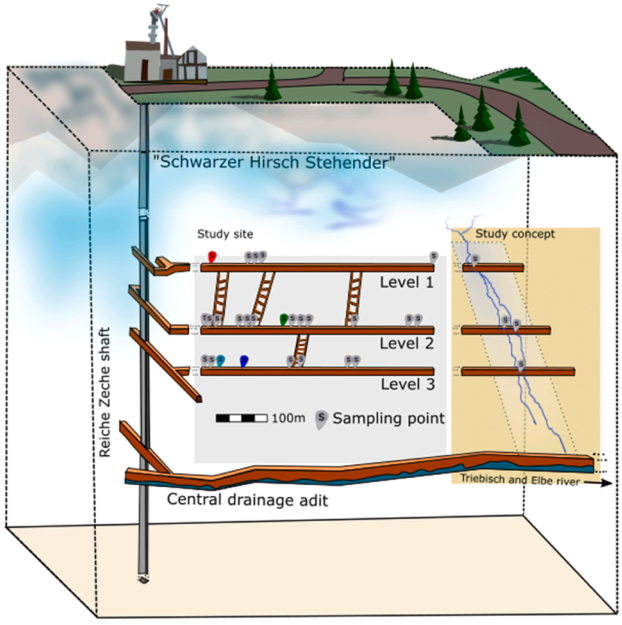


**Fig. 1.** Schematic illustration of study site "Schwarzer Hirsch Stehender" at Reiche Zeiche experimental mine. Samples were collected at 26 sites across three levels, linked through several vertical connections (marked as ladders). Grey inlet shows positions of sites (to scale). Yellow inlet shows concept of the mine water flow system, where water seeps through the former vertically slanted extraction plain in which the three levels are situated. At sites with continuous water flow (site 1 – red, site 2 – green, site 3A – dark blue, and site 3B – light blue) loggers were placed to monitor and quantify flow.

### 2.2. Analytic methods

Water samples were collected in acid-cleaned HDPE bottles that were rinsed with deionized water before usage. In all samples, pH and conductivity were measured (pH 340 and Cond3310 sensors, WTW, Weilheim, Germany). Samples for analysis of dissolved organic and inorganic carbon (DOC, DIC), metal(loid)s, absorbance, and fluorescence analysis were filtered through polyethersulfone filters with a 0.45 µm pore size (Filtropur S, Sarstedt AG & Co. KG, Nümbrecht, Germany) before analysis.

The DOC and DIC concentration of each sample was measured in triplicate and determined using a total organic carbon analyzer (TOC-L series, Shimadzu, Duisburg, Germany). DOC was measured as non-purgeable organic carbon (NPOC) using a high temperature combustion method in which acidified samples were purged with oxygen prior to measurement to remove inorganic carbon. Measurement uncertainty was accounted for by calculating the standard deviation of the triplicate measurements, ensuring the reliability of our data within the instrument's precision limits (variation coefficient $< 2\%$ and standard error $< 0.1$). Metal(oid)s were quantified by inductively coupled plasma optical emission spectroscopy (ICP-OES Optima 5300 DV Spectrometer, PerkinElmer, Rodgau, Germany).

Mine water samples for metal(loid) analyses were acidified with 1 mL of 2% $HNO_3$ and the following metal(loid)s were analyzed: Fe, Zn, As, Cu, Cd, Pb, Al, Ni, and Mn. A solid sample of Reiche Zeche ore and gneiss taken from level 2 of the mine were treated with nitrous-oxide microwave digestion followed by ICP-OES analysis. Using a 2-ray spectrophotometer, UV-Vis spectra for each sample in a 1-cm quartz cuvette were recorded versus deionized water at wavelengths from 200 nm to 700 nm (LAMBDA 365 UV-Vis Spectrophotometer, PerkinElmer, Rodgau, Germany). The spectral slope ratio (Sr) was calculated by dividing the slopes from two wavelength region (275-295nm, 250-400nm), related to DOM average molecular weight (Helms et al., 2008). SUVA254 was calculated by dividing the UV absorbance at the wavelength of 254 nm by the DOC concentration to act as a proxy for DOM aromaticity (Weishaar et al., 2003).

### 2.3. In situ instruments

We positioned water level loggers with barometric reference (Levelogger 5 and Barologger 5, Solinst, Georgetown, ON Canada) at specific sites (site 1 at level 1, site 2 at level 2, sites 3A and 3B at level 3 shown in Fig. 1) to monitor the water levels. At sites 1 and 2 plastic weirs were built. Sites 3A and 3B had natural spillways. With respective manual flow measurements during the sampling campaigns water level-discharge relationships fitting the formula for triangular weirs from Henderson (1996) were established:

$$Q = \frac{8}{15} * C_d * \sqrt[2]{2 * g} * \tan\left(\frac{\alpha}{2}\right) * h^{\frac{5}{2}} \quad (1)$$

where Q is the flow rate (in $m^3\ s^{-1}$), $C_d$ is the discharge coefficient, g is the gravitational constant (9.81 m $s^{-2}$), α is the angle of the lower weir edge (°) and h is the water level above the outlet (m). Before applying the water-level discharge relationship, the 15-minute records were aggregated to 1 hour and processed with a Savitzky-Golay filter to reduce noise in the data.

### 2.4. EEM analysis

Fluorescence of excitation emission scans along with simultaneous absorbance measurements were performed for 320 samples. These samples were selected from the most frequently sampled sites across the three mine levels, where water was consistently present. A 1-cm quartz cuvette was filled with a filtered sample, and fluorescence excitation emission matrix (EEM) spectra were acquired in 0.25 s integration time (Aqualog fluorometer, Horiba Jobin Yvon GmbH, Oberursel, Germany) at an excitation (Ex) range of 240 nm to 450 nm with 3 nm increments and an emission (Em) range of 251.749 nm to 447.627 nm at 4.65 nm increments. The EEMs were corrected for the inner filter effect, Raman normalization, and Rayleigh masking and ultrapure water blanks were subtracted (Wasswa et al., 2019, Sanchez et al., 2020).

All post-processing was done with the DOMFluor toolbox in MATLAB (MathWorks Software R2022b). From the corrected EEMs, fluorescent peak intensities were extracted for all measured samples and PARAFAC was used to analyze the relative distribution of fluorescent components in each sample. During the PARAFAC, two outliers were removed, and the final fluorescent components were validated by split half and residual analyses. The ability of PARAFAC to separate overlapping signals provides deeper analytical insights into the composition and dynamics of DOM quality and allows us to futher reveal patterns between DOM components, metal(loid) variability, and water flow regimes in mine waters. By comparing our results with established data on the DOMopenfluor website (Murphy et al., 2013) and other related studies, PARAFAC facilitates the validation of identified fluorescent components against a broader dataset. Spectral indices, including the humification index (HIX) and the biological index (BIX), were calculated with slight modifications due to available data. The HIX was determined by calculating the ratio of the peak area under emission at 435-480 nm to the peak area under emission at 300-345 nm, using excitation at 255 nm (in place of the standard 254 nm). Similarly, the BIX was calculated as the ratio of emission intensity at 380 nm to the maximum emission intensity at 430 nm, using excitation at 310 nm, with closely matching wavelengths (Em 378.595 nm, Ex 429.151 nm, and Ex 309 nm) utilized to approximate the standard measurements (Zhang et al., 2021).

Our previous analyses provided a comprehensive dataset of physicochemical parameters within the mine drainage system, enabling further detailed statistical analyses.

### 2.5. Statistical analyses

We characterized observed patterns for DOM and metal(loid) interactions using z-score normalization to express concentrations as multiples of standard deviations from the mean. This facilitated the identification and comparison of relative differences and patterns despite varying concentration scales across samples.

Principal Component Analysis (PCA), which reduces data dimensionality while preserving variance, was used to reduce metal(loid) concentration and composition heterogeneity. The factor loadings from the PCA, which presents each metal(loid)s contribution to the cumulative proportion of each principal component, helped to identify which metal(loid)s might be driving the variance in the data. We then linked our metal(loid) concentration data and compositional data by using Spearman rank correlations made with the first two principal components (PC1 and PC2) to explore drivers of composition patterns.

We divided the flow data into two phases to better assess the impact of varying flow regimes on the concentration of metal(loid)s and DOM components. A division between a high flow (February 2$^{nd}$, 2022 – March 31$^{st}$, 2022 and January 1$^{st}$, 2023 – May 31$^{st}$, 2023) and a low flow (April 1$^{st}$, 2022 – December 31$^{st}$, 2022 and June 1$^{st}$, 2023 – August 3$^{rd}$, 2023) period was made based on clear seasonal patterns observed in the input and flow data. To further analyze how variable high flow versus stable low flow conditions influence metal(loid) transport and distribution dynamics, we conducted T-Tests to confirm significant differences among sample means between the high and low flow phases.

Concentration-discharge (C-Q) relationships in log-log space were evaluated to investigate if and why some areas of the mine are over-proportional sources of a certain metal(loid) during high flow, and how the observed behavior is comparable to DOM quantity and quality. We used the slope (β) value as the prime information value for each C-Q relationship and refer to the slope (β) values using C-Q plots. We compared the slope (β) values among each relationship to better

evaluate the process, such as dilution or enrichment, that may be responsible for the observed C-Q behavior.

Generalized linear models, such as multiple regression analysis, were performed with the R 'stats' package (glm function, R Core Team, 2021) and used to best measure the degree of relation between PCA components and certain physiochemical parameters. The multiple $R^2$ value was calculated to assess the proportion of variance explained by the model. Additionally, the Akaike Information Criterion (AIC) was calculated to compare model fits and select the best model based on the trade-off between goodness of fit and model complexity. Plotting was done with the R 'ggplot2' package (R Core Team, 2021; Wickham, 2016).

## 3. Results

### 3.1. Physicochemical parameters and temporal patterns

pH, Electrical Conductivity (EC), metal(loid) concentrations, and DOM quantity and quality parameters were measured in waters from continuously sampled sites in 33 campaigns across all mine levels. Averages and ranges of these physiochemical parameters for each level are shown in Table S1.

Dissolved metal(loid)s tend to increase with depth, and accumulation with depth was highest for dissolved Fe (3 orders of magnitude, Table S1) and Zn (1 order of magnitude, Table S1). Dissolved Fe was the most variable metal across each level (Table S1). Time series analysis of z-score normalized dissolved Fe concentrations reveals distinct temporal patterns (Fig. 2).

The time-series for level 1 exhibits relatively moderate fluctuations

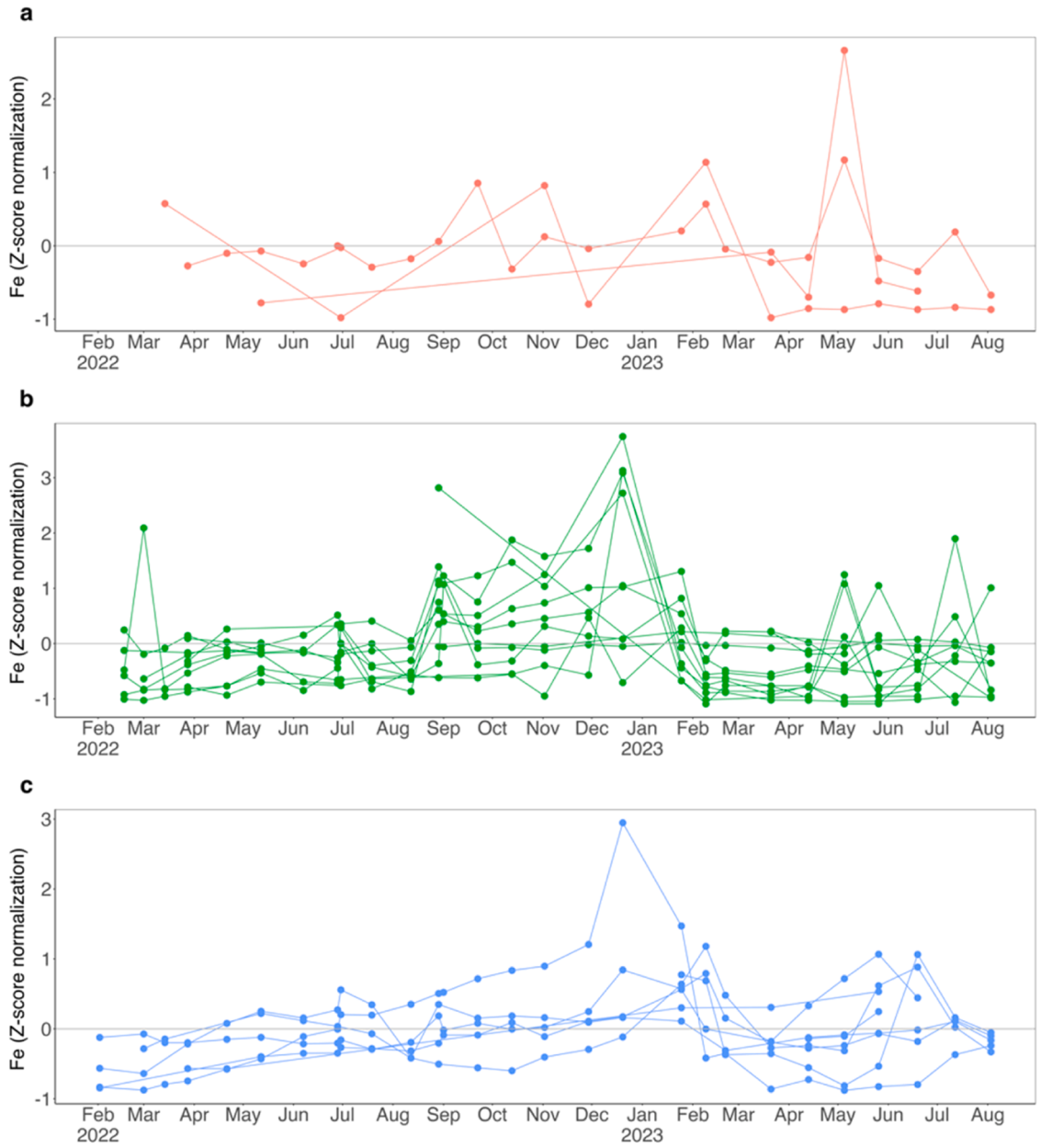


**Fig. 2.** Spatial and temporal dynamics in dissolved Fe concentrations across the mine system. Values are z-scaled, i.e. dissolved Fe concentrations are visualized in standard deviations (SD) away from the site mean. Individual sites are connected by colored lines for level 1 (3 sites, blue, panel a), level 2 (13 sites, green, panel b), and level 3 (8 sites, red, panel c). Points are missing when sites were dry.

throughout the 18-month period, with a notable peak in early 2023. In levels 2 and 3 this dynamic is more pronounced, both showing substantial variability and sites with dominant peaks above 1 SD (10 sites in level 2 and 4 sites in level 3), indicating strong seasonality and potentially event driven pulses in dissolved Fe concentration values. The temporal trends underscore the dynamic nature of the monitored system, reflecting the influence of both periodic and sporadic environmental factors on each site.

### 3.2. Hydrological structure and metal(loid) variations

The hydrological framework of the mine system was the second focus of this study. We measured flow rate (Q) at four sampling sites from February 2022 to August 2023. The observation time was separated into two distinct phases of low flow (LF) and high flow (HF) (Fig. 3a). Within each flow phase, we compared metal(oid) concentrations (z-scaled for each site, T-Test, Fig. 3b-i). During high flow, all metal(oid)s consistently show a reduction in standardized concentrations. Between high and low flow phases, standardized Cd and Zn held the largest mean difference of 0.649 (SE = 0.187) and 0.609 (SE = 0.209), while Al held the smallest mean difference of 0.340 (SE = 0.132). The flow-related concentration changes were tested for significant differences using T-Tests, which was confirmed dilution for all metal(oid)s.

### 3.3. PCA and environmental correlations

PCA was performed with nine variables in 464 mine water samples. Results from the PCA were used to evaluate the metal(loid) variation

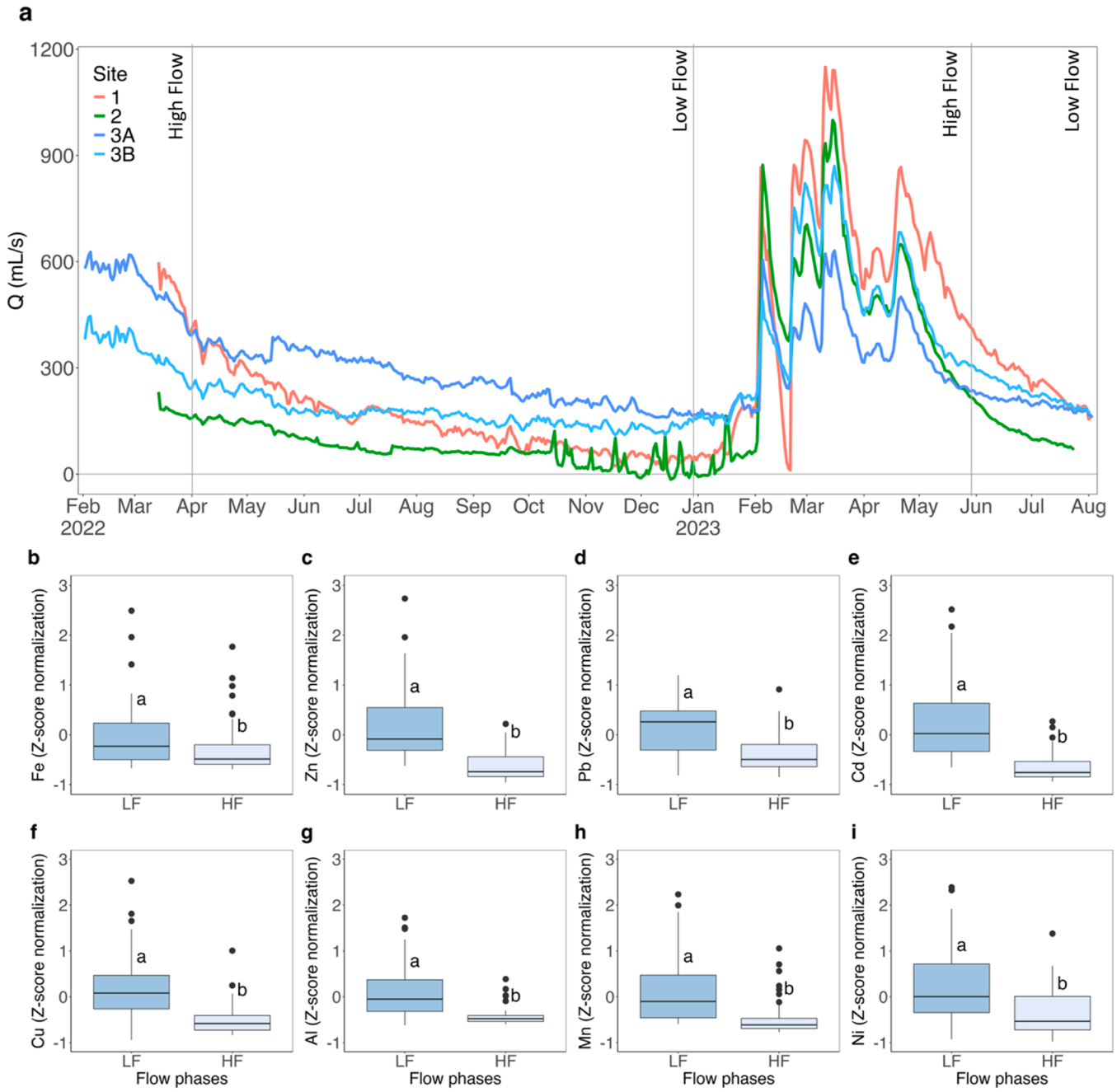


**Fig. 3.** Recorded flow rate at sites 1, 2, 3A, and 3B across time with sections divided by flow phase (light grey line) (panel a) and z-scaled dissolved metal concentrations, Fe, Zn, Pb, Cd, Cu, Al, Mn, and Ni across each flow phase (panels b-i). The blue color boxplot scale refers to the median value of each metal measured (darkest blue = highest median value) and the letters (a and b) above each boxplot indicate significantly different distributions (Tukey HSD test) result.

among level. Only the principal components (PCs) with an eigenvalue greater than or equal to one were considered (Table S2). We observed distinct clustering of sample sites by levels (Fig. 4a), reflecting different metal(loid) signatures between the levels. The PCA ordination plot shows a maximum variance being explained by the first principal component (PC1), which constitutes 42%, and the second principal component (PC2), which accounts for 19.4% of the variance. PC1 was largely defined by the positive loadings for As (2.47) and Ni (2.41) and negative loadings for Al (-1.73) and Zn (-1.53), whereas PC2 contrast samples with high levels of Mn (2.76) and Fe (1.92) against those with high levels of Pb (-1.80) and Zn (-2.62) (Table S2 and Fig. 4a). Composition of solid local samples of gneiss and ore (Table S3), added to the PCA, are distinguished by their positioning relative to the clusters, with ore appearing to be associated with similar PC1 values as sites in levels 2 and 3 whereas gneiss does not follow this pattern.

The variation of PC1 was compared with the physicochemical parameters from Table S1 to identify significant relationships between the variation of metal(loid)s and environmental properties that could be considered as controls. The relationship between acidity (pH) and PC1 (metal(loid) composition) reveals an overall significant and strong monotone relationship ($r_s = 0.894$) (Fig. 4b and S2).

The variance of PC1 versus pH shows that samples from level 3 have a more acidic and compact grouping of pH values, while levels 1 and 2 have a broader range of higher values.

### 3.4. PARAFAC components

Under different discharge conditions and throughout the three levels, most metal(loid)s portrayed variable behaviors. To better constrain the mechanisms underlying these variations, we examined the composition and variability of potential metal(oid)-mobilizing DOM. Therefore, the composition and variability, as analyzed by PARAFAC, revealed that a three-component model could explain the composition of EEMs from all samples (Fig. S5). The first component (C1) features a peak near Ex/Em 252/417 nm, the second component (C2) a peak near Ex/Em 252/347 nm, and the third component (C3) near Ex/Em 267/297 nm. Our PARAFAC model shows components with a Tucker Congruence Coefficient (TCC) $\geq$ 95% similarity to models listed in the OpenFluor database. Given the limited number of published models related to mine water drainage systems, we also compared our PARAFAC model to other relevant studies (Table S7). C2 was more variable across levels in comparison to C1 and C3 (Fig. 5), and increased with level depth. Other DOM proxies, Sr and SUVA254 showed a high degree of variability across time periods and levels, predominantly in levels 2 and 3. (Fig. S1).

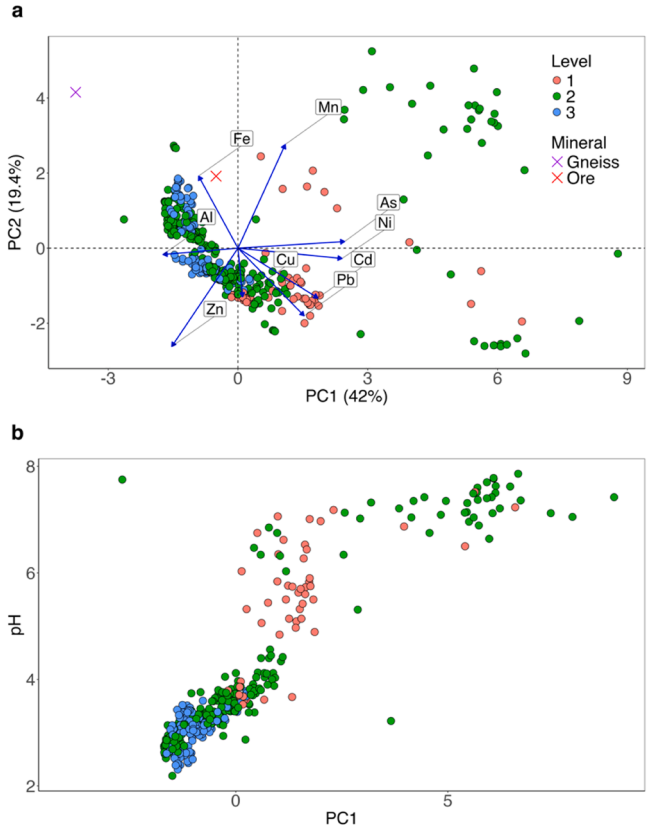


**Fig. 4.** Principal component analysis bi-plot of explanatory metal variables in relation to water sampling sites (points) in each level and mineral samples (crosses) (panel a) and variation of metals from principal component 1 versus pH with points referring to sample sites from each level (panel b).

### 3.5. C-Q relationships

Since most metal(loid)s and DOM components held varying responses to discharge (Fig. 3) or level (Fig.s 2 and 5), their response behavior to flow conditions was tracked using C-Q relationships where flow monitoring permitted. At the four monitored water flow sites (1, 2, 3A, and 3B) we compared the slope (β) of linear regressions between flow and dissolved Fe, Pb, Zn, Al, DOC concentrations, and fluorescent component C2 in log-log space.

C-Q plot slopes are indicative of differences in the processes that affect solute transport and retention. C-Q plot of Fe showed sites 2 and 3B to have more negative slopes (dilution) than sites 1 and 3A, whereas C-Q plot of Al showed sites 2, 3A, and 3B to have similarly high negative slopes. C-Q plots of Zn and DOC showed site 1 to be the unique among sampling sites in its small, near 0 slopes, demonstrating that concentrations are relatively lower yet constant regardless of discharge. Besides the C-Q plot of Pb showing a positive slope for 3A (enrichment), all C-Q plots had negative trends (dilution) for sites below level 1. DOC quantity and C2 Fmax showed to have different responses to changing flow regimes with fluorescent component C2 being most variable across changes in discharge (Fig. 6f).

### 3.6. Correlations between PC's and DOM characteristics

To assess the effect of DOM characteristics on metal(loid) mobility, we used Spearman's rank correlation to examine the association between various DOM indices and PC1, which encapsulates the majority of the variance in the metal(loid) data (Fig. 7). We found a weak negative relationship between PC1 and DOC ($r_s$ = -0.243) and a significant negative relationship between PC1 and C2 ($r_s$ = -0.910). The relationship between PC1 and Sr showed to have a strong negative relationship ($r_s$ = -0.744), while PC1 and SUVA254 showed to have a weak negative relationship ($r_s$ = -0.193) (Table S5).

## 4. Discussion

### 4.1. Variation of metal(loid) concentrations across mine levels

Our investigation into seasonal and spatial variations in water quality within the Reiche Zeche mine, and the dynamics of mine water DOM on metal(loid) mobility, reveals critical insights into the environmental behavior of these elements. pH, DOC and metal(loid) concentrations displayed variations among the levels, with level 3 showing the highest average concentration for all $H^+$ (pH 2.3-3.8), and all measured metal(loid)s, particularly Fe and Zn (Table S1). This is consistent with many reports of increased metal release from environments with lower pH (Butler 2009; Gambrell et al., 1991; Dijkstra et al., 2004), especially of Fe (Behera & Shukla, 2015; Khaledian et al., 2017; Zhu et al., 2021). Similar to metal(loid) concentrations, DOC concentrations increased from top to bottom levels, but less intensively with

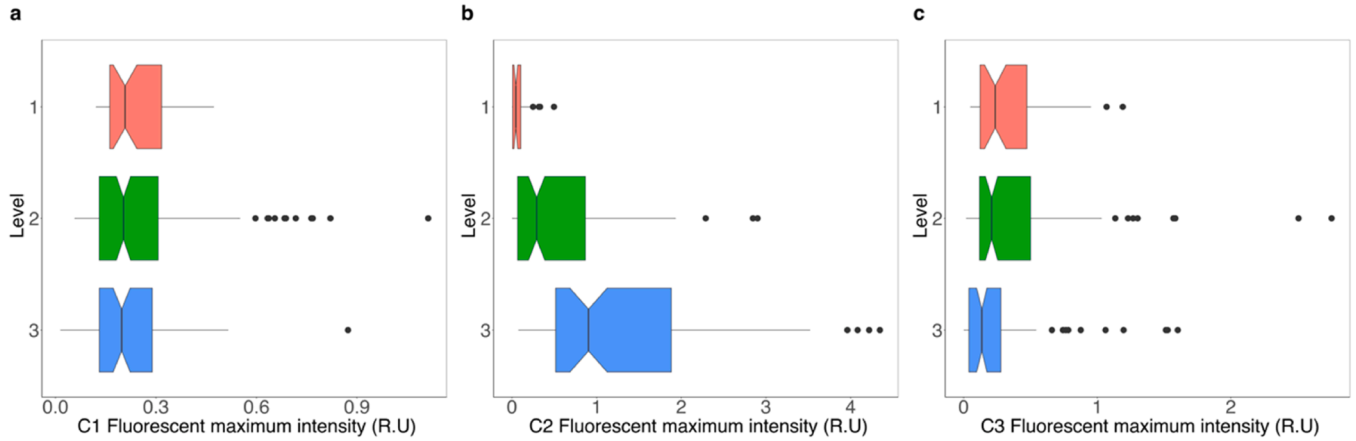


**Fig. 5.** Fluorescence component maximum intensities from PARAFAC (panel a – C1, panel b – C2, panel c – C3) for water samples collected in levels 1 (n=48), 2 (n=174), and 3 (n=98), expressed in in Raman units (R.U.).

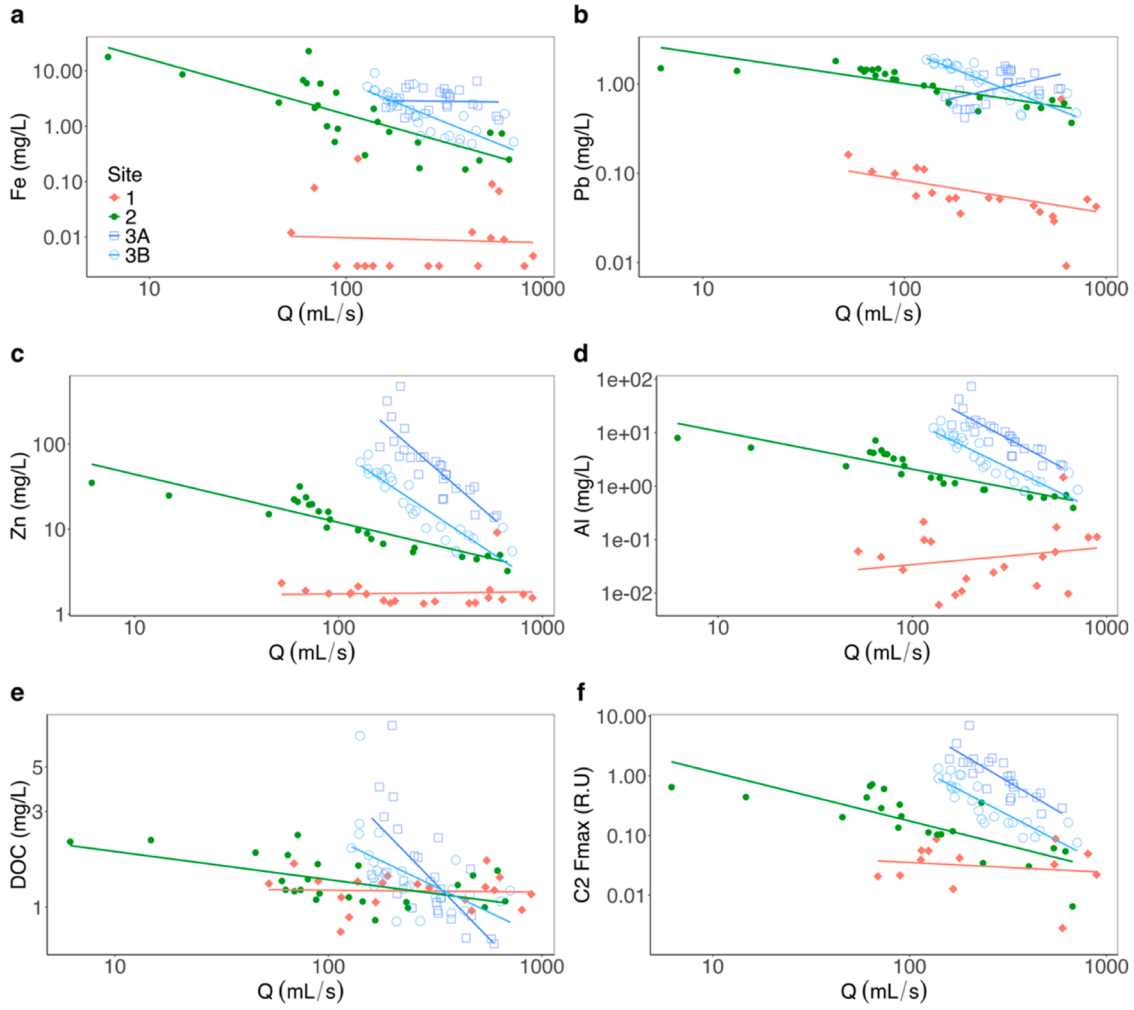


**Fig. 6.** Concentration-discharge relationships for four monitored flow sites (1, 2, 3A, and 3B) for Fe (a), Pb (b), Zn (c), Al (d), DOC (e), and the fluorescent component C2 of DOM, (Fmax, panel f) with (log-log) linear regression line for each site (1 – blue, 2 – purple, 3A – dark blue, 3B – light blue). Analyses include 19-26 samples per site for measured concentrations and 13-23 samples for measured fluorescence values.

average values of 1.1 mg/L, 1.4 mg/L, and 1.6 mg/L (Levels 1, 2 and 3).

By example of Fe, we confirm an increase in metal concentration corresponding with the depth and associated DOC and acidity across levels: Average Fe concentration (mean ± SE) reached from 0.052 mg/L ± 0.008 at level 1, via 8.0 mg/L ± 0.80 to 31 mg/L ± 7.2 at level 3. Baake (2000) found that several months after the flooding of Reiche Zeche in 1971, the low pH conditions led to an increase in dissolved Fe and Zn concentrations, as the acidic water enhanced the leaching of these metals from surrounding (secondary) minerals. Reduction of the dimensions of chemical composition by PCA analysis (Fig. 4) showed

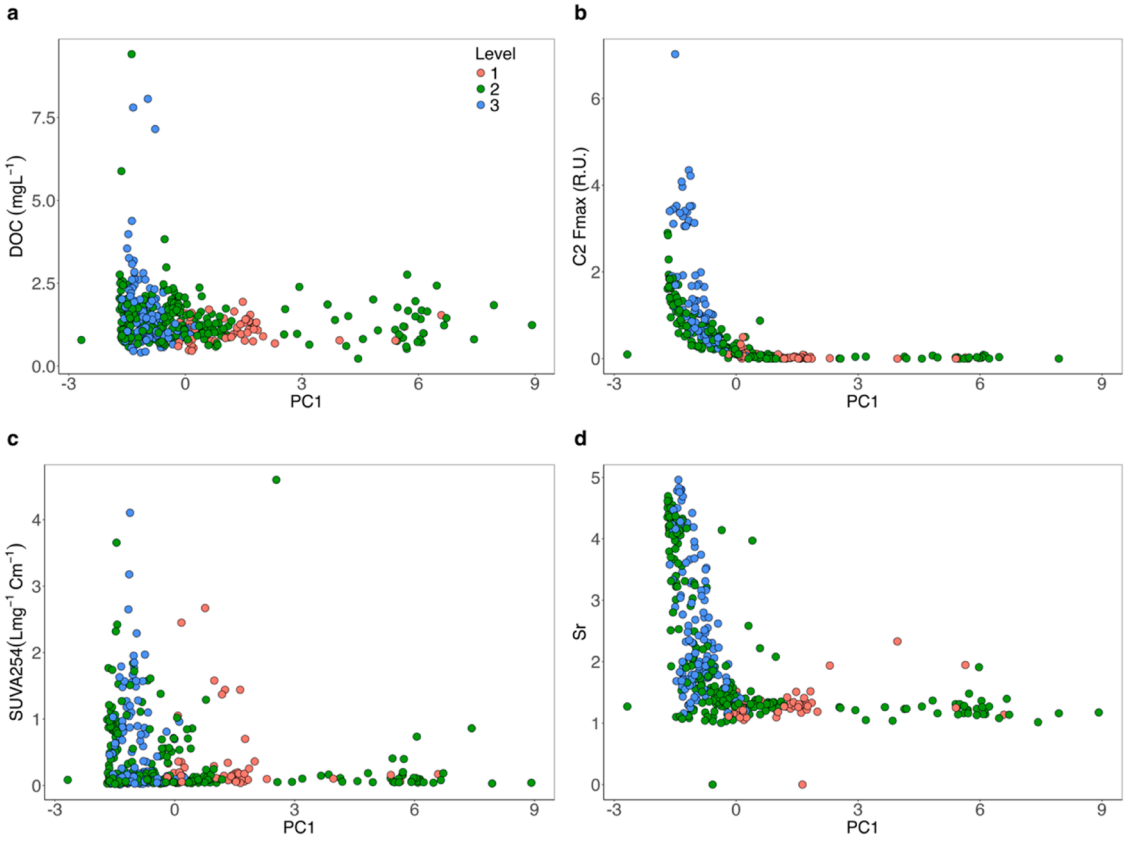


**Fig. 7.** Variation of metal(loid)s from principal component 1 versus presumed biogeochemical controls, DOC (panel a), fluorescent component C2 (panel b), SUVA254 (panel c), and spectral slope ratio (panel d). Points refer to samples from each level.

that the variability of Fe, and other metal(loid)s to be partially represented by the first principal component (PC1). The PCA biplot showed that most sites at level 1 had high positive values for PC1 and are characterized by higher concentrations of Cd and Pb, while the PC1 for water sample sites at levels 2 and 3, and the ore mineral sample were more influenced by Zn, Al, and Fe concentrations. By exploring possible drivers of this variability, we found that PC1 was strongly and positively correlated to pH (Fig. 4b and Table S5), suggesting that samples with higher PC1 values might represent a metal(loid) profile associated with a higher pH. The correlation of pH with Fe, Zn, and Al from PC1 additionally indicate that these metals may be released from the ore under a pH change to lower values.

### 4.2. Seasonal variations in metal(loid) concentrations

A temporal analysis revealed seasonal variations, particularly marked concentration decreases in January/February 2023 (Figs. 2a-c and S2). The highly dynamic spatial and temporal patterns likely emanate from hydrometeorological conditions influencing the water availability, and differential rates of metal release from solid or sedimentary matrices, influencing ambient metal(oid) concentration (Pohle et al., 2021). More water in a porous mine system may further facilitate the dynamic connection and disconnection of metal(oid)-releasing areas under elevated water availability, similar to porous soil systems (Jackisch & Zehe, 2018). We found seasonal flow regime patterns, with significantly higher metal(loid) concentrations during low flow phases (Fig. 3b-i), signifying dilution scenarios of different extend for all metals. To trace periodicity of these phases, we examined local rainfall data but observed no direct impact visually on the water flow within the mine (Fig. S3). Instead, flow dynamic shifts only with large additional surface water fluxes as during snowmelt, for example observed in the winter of 2022/2023 (Fig. S3). The flow timeseries and C-Q relationships suggest a hydrochemical regime that features episodic yet regular discharges of fluids, with lower but non-conservatively diluted metal(oid) concentrations (Nordstrom, 2011).

### 4.3. Limitations of metal(loid) release during high flow phases

C-Q relationships revealed that non-conservative behavior during increased water availability points to the transport limitation of some metal(oid) releasing areas within the mine. Soluble salts and secondary minerals form on surfaces during dry periods and when significant flow increases occur, these materials can dissolve (Nordstrom, 2011; Hendrickson and Krieger, 1960; Gyzl and Banks, 2007). Flow increase further leads to dynamic dilution in parallel with changes in metal concentrations of various degree (Nordstrom, 2011). Within the mine, various sometimes disconnected and semi-connected water bodies, along with the patchy distribution of ore, create complex and variable flow paths of varying activity. During high flow conditions, it is likely that these different flow paths, possibly including those from previously dry parts of the mine, become activated, allowing Zn to be mobilized from trace ore materials embedded in left-over material or unrecovered ore within the mine. Slope values for the C-Q relationship for Zn, for example, showed more decreasing concentrations with flow at sites 3A ($\beta$=-2.15 $\pm$ 0.32) and 3B ($\beta$=-1.46 $\pm$ 0.13) than at sites 2 ($\beta$=-0.56 $\pm$ 0.06) and 1 ($\beta$=-0.093 $\pm$ 0.04). Such response factors infer that there may be excess reservoirs of Zn that are tapped during the high flow season at sites 1 and 2. Therefore, Zn mobilization rates at sites 1 and 2 hinge not solely on water flux but also on the flow path and complex source dynamics. The PCA supports this notion, showing that RZ ore had an elemental composition that was responsible for clustering the mine water samples (Fig. 4). The strong connection between the elemental makeup of the ore and the drivers of metal(loid) variability in the mine water helps interpret the observed C-Q relationship patterns of Zn and

Al. The C-Q relationship for Al showed similar patterns as Zn, such that at sites 3A (β=-2.00 ± 0.31) and 3B (β=-1.60 ± 0.15) concentrations decreased faster with flow than at sites 1 (β=0.100 ± 0.3) and 2 (β=-0.70 ± 0.07). This suggests that there may be more water flowing from distributed sources in areas of active ore leaching, where C-Q relationships then do not present conservative dilution scenarios. Pohle et al. (2021) assumed solute source limitation and solute transport limitation, the latter occurring when the carrying capacity of the transport medium (like water) constrains export, despite ample substance at the source.

### 4.4. Impact of flow regimes on metal(loid) loads

Non-proportional dilution during high flow phases is also leading to a disproportionally larger share of these periods to the annual metal (loid) load. Comparison across seasons revealed that the Zn loads are exported primarily during the high flow regime (high flow represents 92.9% of yearly Zn load in one third of the year (38.3% of the year's days) at site 1, 52.8% at site 2, 34.8% at site 3A, and 36.5% at site 3B) (Table S8). This imbalance supports an additional contributing mechanism, such as mobilization of stored solutes. The degree of this intermittent behavior is site and metal(loid) specific. Hydrodynamic factors, such as water flow and volume, along with geological features, influence these variations in metal(loid) dispersion and concentration (Rose et al., 2018).

### 4.5. Role of DOM in metal(loid) release

Beyond hydrodynamic drivers, we also explored the role of biogeochemical factors, such as DOM, for metal(loid) release. Mean DOM-C concentrations in mine water ranged from 1.1 mg/L to 1.6 mg/L across the three levels, similar to groundwater values (Harjung et al., 2023), possibly due to shared sources of organic matter and hydrological connectivity. Although DOM may support metal(loid) release through complexation (Cornu et al., 2011), we could not confirm that DOC concentration alone is a driver for metal(loid) release (Fig. 7a). However, shifts in DOM quality between levels (Fig. 5b), and strong correlations with metal(loid) composition and abundance were observed (Fig. 7b-d). The three DOM components from the PARAFAC model were compared with the excitation/emission characteristic peaks from studies in OpenFluor with TCC>95% and other studies related to mine waters to best characterize our components (Table S7). Component 1 (C1), identified as humic-like DOM (Catalán et al., 2018; Coble 1996, 2007), had low abundance across all levels (Fig. 5a) but a higher and more significant correlation with PC2 than PC1 (Table S5). This component, associated with large aromatic molecules (Garcia et al., 2015), decreases in fluorescent intensity upon acidification due to changes in hydroxyl and carboxyl groups (Kulkarni et al., 2019). Decreases in HIX values across greater mine depths confirms a lesser degree of humification and presence of less aromatic material (Fig. S4). However, a significant correlation with PC1 and PC2 (Table S5) suggests that humic substances in a mine system, which can be sourced from the leaching of surface sources through water percolation, may play a role in metal(loid) variability. Component 3 (C3) is most likely associated with proteinaceous material and tyrosine-like fluorophores (DeFrancesco & Gueguen, 2021; Harsha et al., 2023; Yamashita and Tanoue, 2003), showing no significant variation across levels. Component 2 (C2) most likely represents a fluorescence region dominated by tryptophan-like fluorophores (Wang et al., 2020), low aromatic content, low molecular weight, and potentially bioreactive chemical species (D'Andrilli & McConnell, 2021). The peak of tryptophan is usually detected at Ex/Em = 278/340 nm (Kowalczuk et al., 2003) and our characteristic peaks of C2 were close to those of protein-like substances (Table S7). Studies related to mine drainage waters confirm that component 2 is most similar to tryptophan-like fluorescence (Li et al., 2024; Hongxia et al., 2014) or a fluorescence region dominated by the production of soluble microbial products (SMP) (Zhang et al., 2021). Therefore, it is possible that areas with high intensities of C2 may be influenced by microbial processes so that C2 can be better referred to as microbial-like DOM. An increase in mean Sr values with greater depths (Table S1) confirms the presence of low molecular weight substances, which are associated with high microbial activity, further suggesting that C2 may be properly characterized as more bio-derived DOM. There was a clear difference in C2 abundance across levels (Fig. 5), implying more DOM molecules of these chemical composition in deeper areas of the mine. BIX values presented a similar pattern with greater depths (Fig. S4), suggesting the presence of microbial activity (Li et al., 2024). Therefore, higher C2 abundance may imply enhanced microbial activity, greater ambient production and accumulation of DOM, and potentially more labile and bioreactive DOM species present as depth increases. These observations collectively support the classification of C2 as microbial-like DOM, with its abundance increasing with depth, aligning with the chemical data that suggests a coupled abiotic-biotic process of ore dissolution.

### 4.6. Microbial influence on metal(loid) dynamics

The role of microbial processes proves to play a greater role in areas of the mine, such that the observed patterns suggest that acidity and microbial DOM are closely linked to sulfide dissolution in mine drainage waters: Haferburg et al. (2022) found that sulfur-oxidizing bacteria (SOB), such as *Thiomonas* and *Sulfuriferula*, generate acidity through sulfide oxidation in mine environments. This increased acidity correlates with microbial DOM production, particularly in areas with high C2 fluorescence intensities, suggesting that sulfide dissolution not only drives acidity but also stimulates microbial activity and DOM dynamics. PCA further elucidates these relationships, with PC1 showing a negative asymptotic relationship with the microbial-like C2 component, as well as with Sr and BIX values (Fig. 7b, 7d and Fig. S5a), with values shifting less as samples are collected nearer to the surface (level 1). However, C2 portrayed the most significant and strongest monotone relationship with PC1, indicative of metal(loid) variability (Table S3). A higher amount of Fe, Zn and Al co-occur with larger masses of this microbial proxy (Fig. 7b and Table S4). Multiple regression analysis further shows a strong, statistically significant relationship between PC1, pH, and C2 (p-values < 0.001). The model explained a substantial portion of the variance in PC1 (multiple $R^2 = 0.789$) and held the best fit model (AIC = 820) in comparison with models using C1 and C3 in place of C2. Four models between PC1, pH, and different DOM component combinations were additionally performed, but all explained a lower portion of the variance in PC1 and presented higher AIC values, suggesting that the most important predictors are indeed pH and C2. This underscores the significant role of acidophile microbial processes in shaping the organic profile of the mine drainage water and influencing metal(loid) dynamics (Haferburg et al., 2022).

### 4.7. DOM and metal(loid) interactions under varying hydrological conditions

C-Q relationships between DOM and water discharge at the monitored sites reveal important insights into DOM and metal(loid) interactions in mine drainage waters. DOC quantity and water discharge relationship at sites 1 and 2 showed stable DOC concentrations, with β values of -0.011 and -0.14, suggesting that DOM in receiving waters is loaded outside of the mine system, for example in percolated soils above. Opposed to bulk DOM concentration, we observed a dependence of DOM composition on flow. Negative C-Q relationships for C2 at sites 2 (β = -0.87 ± 0.14), 3B (β = -1.64 ± 0.21), and 3A (β = -2.03 ± 0.33) indicate high local variability in metal-DOM interplay. At site 3A, high flow periods are characterized by relatively stable concentrations of dissolved Fe and large decreases in microbial DOM (C2), suggesting a setup in which high flow activates reservoirs of microbially-mobilized metal. At position 3B, high flow periods portray a strong decrease of

both dissolved Fe and C2, indicating dilution and reduced microbial mobilization during high flow. The observed patterns support the idea that dissolved Fe may be released from ore bodies, and this release is closely tied to microbial processes. These findings highlight the dynamic nature of DOM mobilization and its interaction with metal(loid)s under varying hydrological conditions. Baker and Banfield (2003) highlighted that the production of acidity through microbial processes not only mobilizes metal(loid)s but also creates conditions that sustain further microbial activity, creating a cycle of metal mobilization. Other factors, such as redox potential, ionic strength, pH, and competing ions, characteristic for different mine water sources, sediments, and chemical interaction effects can also influence subsequent metal(loid) solubility and transport (Butler, 2009). Previous studies indicate that DOM components in mine water may alter metal(loid) binding affinities and thus the stability of metal complexes (Hongxia et al., 2014; Zhang et al., 2021). Our findings build on these concepts by demonstrating the dynamic nature of DOM mobilization and its interaction with metal(loid)s under varying hydrological conditions, providing key insights for improving internal pollution control strategies and mine water management.

## 5. Conclusion

Our empirical analyses reveal that metal(loid) concentrations are intricately tied to the hydrological behavior of the system, with seasonal variations and intermittent events playing a pivotal role, such that metal (loid) concentrations and DOM proxies exhibit pronounced fluctuations across various mine depths, with some sites portraying a notable excess metal(loid) presence during high flow periods. The observed dynamics in DOM demonstrate a significant impact on the mobility and distribution of metal(loid)s in the mine waters. Notably, there are strong correlations between metal(loid) variability and both microbial DOM and pH. The linkage between pH and metal(loid) variability observed in PC1, coupled with the dynamic changes in fluorescent DOM and C-Q relationships, points to a complex system where ore-derived metal(loid)s are mobilized under specific hydrological conditions, sustaining microbial activity that continues to influence metal(loid) mobilization. These relationships highlight the crucial role of microbial processes in contributing to the observed metal(loid) behavior. The study's insights into the intricate interplay of biogeochemical processes in mining-impacted environments underscore the critical need for protecting downstream ecosystems, which are often the silent receivers of mine drainage impacts.

## CRediT authorship contribution statement

**Anita Alexandra Sanchez:** Writing – review & editing, Writing – original draft, Methodology, Investigation, Formal analysis, Data curation, Conceptualization. **Karl Haas:** Investigation, Data curation, Conceptualization. **Conrad Jackisch:** Writing – review & editing, Formal analysis, Conceptualization. **Sabrina Hedrich:** Writing – review & editing, Validation. **Maximilian P. Lau:** Writing – review & editing, Validation, Supervision, Conceptualization.

## Declaration of competing interest

The authors declare that they have no known competing financial interests or personal relationships that could have appeared to influence the work reported in this paper.

## Data availability

Data will be made available on request.

## Acknowledgements

This work, under the project "Source related control and treatment of Saxon mining water", was funded by the Dr. Erich-Krüger Foundation. We acknowledge Dr. Alexander Pleßow for support with laboratory equipment and previous Reiche Zeche mineral data, Prof. Helmut Mischo and Stephan Leibelt for training and access to the Research Mine, and Dr. Andreas Kluge and Dr. Nils Hoth for providing an excellent jumpstart to the mine system. We would also like to thank the laboratory staff, Thurit Tschöpe, Marius Stoll, Claudia Malz, Eva Fischer, and Lena Grundmann, for their assistance with sample measurements, and Lena Herzig for her assistance with mine water collection.

## Supplementary materials

Supplementary material associated with this article can be found, in the online version, at doi:10.1016/j.watres.2024.122336.

## References

Aguilar-Garrido, A., Paniagua-López, M., Sierra-Aragón, M., Martínez Garzón, F.J., Martín-Peinado, F.J., 2023. Remediation potential of mining, agro-industrial, and urban wastes against acid mine drainage. Sci. Rep. 13 (1), 12120. https://doi.org/10.1038/s41598-023-39266-4.

Aguilera, R., Melack, J.M., 2018. Concentration-discharge responses to storm events in coastal california watersheds. Water. Resour. Res. 54 (1), 407–424. https://doi.org/10.1002/2017WR021578.

Arenas-Lago, D., Andrade, M.L., Lago-Vila, M., Rodriguez-Seijo, A., Vega, F.A., 2014. Sequential extraction of heavy metals in soils from copper mine: distribution in geochemical fractions. Geoderma 230–231, 108–118.

Baker, B.J., Banfield, J.F., 2003. Microbial communities in acid mine drainage. FEMS *Microbiol. Ecol* 44, 139–152. https://doi.org/10.1016/s0168-6496(03)00028-x.

Basu, N.B., Thompson, S.E., Rao, P.S.C., 2011. Hydrologic and biogeochemical functioning of intensively managed catchments: A synthesis of top-down analyses. Water. Resour. Res. 47 (10) https://doi.org/10.1029/2011WR010800.

Behera, S.K., Shukla, A.K., 2015. Spatial distribution of surface soil acidity, electrical conductivity, soil organic carbon content and exchangeable potassium, calcium and magnesium in some cropped acid soils of India. Land. Degrad. Dev. 26, 71–79. https://doi.org/10.1002/ldr.2306.

Bieroza, M.Z., Heathwaite, A.L., 2015. Seasonal variation in phosphorus concentration-discharge hysteresis inferred from high-frequency in situ monitoring. J. Hydrol. (Amst) 524, 333–347. https://doi.org/10.1016/j.jhydrol.2015.02.036.

Bracken, L., Wainwright, J., Ali, G., Tetzlaff, D., Smith, M., Reaney, S., Roy, A., 2013. Concepts of hydrological connectivity: Research approaches, pathways and future agendas. Earth. Sci. Rev. 119, 17–34. https://doi.org/10.1016/j.earscirev.2013.02.001.

Butler, B.A., 2009. Effect of pH, ionic strength, dissolved organic carbon, time, and particle size on metals release from mine drainage impacted streambed sediments. Water. Res. 43 (5), 1392–1402. https://doi.org/10.1016/j.watres.2008.12.009.

del Catalán, N., Casas-Ruiz, J.P., Arce, M.I., Abril, M., Bravo, A.G., Campo, R., Estévez, E., Freixa, A., Giménez-Grau, P., González-Ferreras, A.M., Gómez-Gener, Ll., Lupon, A., Martínez, A., Palacin-Lizarbe, C., Poblador, S., Rasines-Ladero, R., Reyes, M., Rodríguez-Castillo, T., Rodríguez-Lozano, P., Sanpera-Calbet, I., Tornero, I., Pastor, A., 2018. Behind the Scenes: Mechanisms Regulating Climatic Patterns of Dissolved Organic Carbon Uptake in Headwater Streams. Glob. Biogeochem. Cycles 32, 1528–1541. https://doi.org/10.1029/2018gb005919.

Coble, P.G., 1996. Characterization of marine and terrestrial DOM in seawater usingexcitation-emission matrix spectroscopy. Mar. Chem. 51 (4), 325–346. https://doi.org/10.1016/0304-4203(95)00062-3.

Coble, P.G., 2007. Marine optical biogeochemistry: the chemistry of ocean color. Chem. Rev. 107, 402–418.

Core Team, R, 2021. R: A language and environment for statistical computing. R Foundation for Statistical Computing. Vienna, Austria. https://www.R-project.org.

Cornu, J.Y., Schneider, A., Jezequel, K., Denaix, L., 2011. Modelling the complexation of Cd in soil solution at different temperatures using the UV-absorbance of dissolved organic matter. Geoderma 162. https://doi.org/10.1016/j.geoderma.2011.01.005.

Cravotta III., C.A., Goode, D.J., Bartles, M.D., Risser, D.W., Galeone, D.G, 2014. Surface water and groundwater interactions in an extensively mined watershed, upper Schuylkill River, Pennsylvania, USA. Hydrol. Process. 28 (10), 3574–3601. https://doi.org/10.1002/hyp.9885.

D'Andrilli, J., McConnell, J.R., 2021. Polar ice core organic matter signatures reveal past atmospheric carbon composition and spatial trends across ancient and modern timescales. J. Glaciol. 67, 1028–1042. https://doi.org/10.1017/jog.2021.51.

DeFrancesco, C., Gueguen, C., 2021. Long-term trends in dissolved organic matter composition and its relation to sea ice in the Canada Basin, Arctic Ocean (2007-2017). J. Geophys. Res.: Oceans 126. https://doi.org/10.1029/2020JC016578.

Dhir, B., 2018. Biotechnological Tools for Remediation of Acid Mine Drainage (Removal of Metals from Wastewater and Leachate). Elsevier: Bio-Geotechnol. Mine Site Rehabil. 67–82.

Dijkstra, J.J., Meeussen, J.C.L., Comans, R.N.J., 2004. Leaching of heavy metals from contaminated soils: An experimental and modeling study. Environ. Sci. Technol. 38, 4390–4395.
Durães, N., Bobos, I., da Silva, E.F., 2017. Speciation and precipitation of heavy metals in high-metal and high-acid mine waters from the Iberian Pyrite Belt (Portugal). Environ. Sci. Pollut. Res. 24 (5), 4562–4576. https://doi.org/10.1007/s11356-016-8161-4.
Fest, P.M.J., 2007. Proton buffering and metal mobility in Dutch sandy soils: modeling laboratory and field data. [Doctoral dissertation]. Wageningen University. ISBN: 978-90-8504-689-9.
Gambrell, R.P., Wiesepape, J.B., Patrick, W.H., Duff, M.C., 1991. The effects of pH, redox, and salinity on metal release from a contaminated sediment. Water. Air. Soil. Pollut. 57–58, 359–367.
Garcia, R.D., Reissig, M., Queimaliños, C.P., Garcia, P.E., Dieguez, M.C., 2015. Climate-driven terrestrial inputs in ultraoligotrophic mountain streams of Andean Patagonia revealed through chromophoric and fluorescent dissolved organic matter. Sci. Total Environ. 521–522, 280–292. https://doi.org/10.1016/j.scitotenv.2015.03.102.
Grande, J.A., Santisteban, M., Torre, M.L.de la, Fortes, J.C., Miguel, E.de, Curiel, J., Dávila, J.M., Biosca, B, 2018. The paradigm of circular mining in the world: the iberian pyrite belt as a potential scenario of interaction. Environ. Earth. Sci. 77 https://doi.org/10.1007/s12665-018-7577-1.
Gyzl, G., Banks, D., 2007. Verification of the "first flush'' phenomenon in mine water from coal mines in the Upper Silesian Coal Basin, Poland. J. Contam. Hydrol. 92, 66–86.
Haferburg, G., Krichler, T., Hedrich, S., 2022. Prokaryotic communities in the historic silver mine Reiche Zeche. Extremophiles. 26 (1) https://doi.org/10.1007/s00792-021-01249-6.
Harjung, A., Schweichhart, J., Rasch, G., Griebler, C., 2023. Large-scale study on groundwater dissolved organic matter reveals a strong heterogeneity and a complex microbial footprint. Sci. Total Environ. 854, 158542 https://doi.org/10.1016/j.scitotenv.2022.158542.
Harsha, M.L., Redman, Z.C., Wesolowski, J., Podgorski, D.C., Tomco, P.L., 2023. Photochemical formation of water-soluble oxyPAHs, naphthenic acids, and other hydrocarbon oxidation products from Cook Inlet, Alaska crude oil and diesel in simulated seawater spills. Environ. Sci.: Adv. 2, 447–461. https://doi.org/10.1039/d2va00325b.
Hedrich, S., Jackisch, C., Hofmann, M., Sanchez, A.A., Haas, K., Gogesch, S., Lau, M.P., 2022. Navigationshilfen zur ursprungsnahen Verminderung von Wasserkontamination im Altbergbau. Acamonta 29.
Helms, J.R., Stubbins, A., Ritchie, J.D., Minor, E.C., Kieber, D.J., Mopper, K., 2008. Absorption spectral slopes and slope ratios as indicators of molecular weight, source, and photobleaching of chromophoric dissolved organic matter. Limnol. Oceanogr. 53 (3), 955–969.
Henderson, Francis Martin. (1966.): Open channel flow /: Macmillan.
Hendrickson, G.E., Krieger, R.A., 1960. Relationship of Chemical Quality of Water to Stream Discharge in Kentucky. Internat. Geol. Cong. XXI Session 1, 66–75. Part.
Holland, A., Stauber, J., Wood, C.M., Trenfield, M., Jolley, D.F., 2018. Dissolved organic matter signatures vary between naturally acidic, circumneutral and groundwater-fed freshwaters in Australia. Water. Res. 137, 184–192. https://doi.org/10.1016/j.watres.2018.02.043.
Hongxia, Y., Jinxu, G., Wei, L., Keyan, T., 2014. Investigating the composition of dissolved organic matter in natural water in rare earth mine using EEM-PARAFAC analysis. Environ. Sci.: Process. Impacts 16, 2527–2535. https://doi.org/10.1039/c4em00380b.
Hunsaker, C.T., Johnson, D.W., 2017. Concentration-discharge relationships in headwater streams of the Sierra Nevada, California. Water. Resour. Res. 53 (9), 7869–7884. https://doi.org/10.1002/2016WR019693.
Jackisch, C., Zehe, E., 2018. Ecohydrological particle model based on representative domains. Hydrol. Earth. Syst. Sci. 22 (7), 3639–3662. https://doi.org/10.5194/hess-22-3639-2018.
Kalonji-Kabambi, A., Demers, I., Bussière, B., 2020. Reactive transport modeling of the geochemical behavior of highly reactive tailings in different environmental conditions. Appl. Geochem. 122 https://doi.org/10.1016/j.apgeochem.2020.104761.
Kefeni, K.K., Msagati, T.A.M., Mamba, B.B., 2017. Acid mine drainage: Prevention, treatment options, and resource recovery: A review. J. Clean. Prod. 151, 475–493.
Khaledian, Y., Pereira, P., Brevik, E.C., Pundyte, N., Paliulis, D., 2017. The influence of organic carbon and pH on heavy metals, potassium, and magnesium levels in Lithuanian pools. Land Degrad. Develop 28, 345–354.
Kowalczuk, P., Cooper, W.J., Whitehead, R.F., Durako, M.J., Sheldon, W., 2003. 809 Characterization of CDOM in organic rich river and surrounding coastal ocean in the 810 South Atlantic Bight. Aquat. Sci. 65 (4), 384–401.
Kulkarni, H., Mladenov, N., Datta, S., 2019. Effects of acidification on the optical properties of dissolved organic matter from high and low arsenic groundwater and surface water. Sci. Total Environ. 653, 1326–1332. https://doi.org/10.1016/j.scitotenv.2018.11.040.
Li, F., Wei, L., Liu, Y., Deng, H., Cui, J., Wang, J., Xiao, T., 2024. Characterization of dissolved organic matter in rivers impacted by acid mine drainage: Components and complexation with metals. Sci. Total Environ. 926, 171960 https://doi.org/10.1016/j.scitotenv.2024.171960.
Lintern, A., Webb, J.A., Ryu, D., Liu, S., Waters, D., Leahy, P., 2018. What are the key catchment characteristics affecting spatial differences in riverine water quality? Water. Resour. Res. 54 (10), 7252–7272. https://doi.org/10.1029/2017WR022172.
McKnight, D.M., Boyer, E.W., Westerhoff, P.K., Doran, P.T., Kulbe, T., Andersen, D.T., 2001. Spectrofluorometric characterization of dissolved organic matter for indication of precursor organic material and aromaticity. Limnol. Oceanogr. 46 https://doi.org/10.4319/lo.2001.46.1.0038.
Merino, N., Jackson, T.R., Campbell, J.H., Kersting, A.B., Sackett, J., Fisher, J.C., Bruckner, J.C., Zavarin, M., Hamilton-Brehm, S.D., Moser, D.P., 2022. Subsurface microbial communities as a tool for characterizing regional-scale groundwater flow. Sci. Total Environ. 842 https://doi.org/10.1016/j.scitotenv.2022.156768.
Murphy, K.R., Stedmon, C.A., Wenig, P., Bro, R., 2013. OpenFluor — an online spectral library of auto-fluorescence by organic compounds in the environment. Anal. Methods 6 (3), 658–661.
Nascimento, S.C., Cooke, D.R., Townsend, A.T., Davidson, G., Parbhakar-Fox, A., Cracknell, M.J., Miller, C.B., 2023. Long-Term Impact of Historical Mining on Water Quality at Mount Lyell, Western Tasmania, Australia. Mine Water. Environ. https://doi.org/10.1007/s10230-023-00943-5.
Nordstrom, D.K., 2008. Questa baseline and pre-mining ground-water quality investigation. 25. summary of results and baseline and Pre-mining Ground-water Geochemistry, Red River Valley, Taos County, New Mexico, 2001–2005. US Geol. Surv. Prof. Paper 1728.
Nordstrom, D.K., 2011. Hydrogeochemical processes governing the origin, transport and fate of major and trace elements from mine wastes and mineralized rock to surface waters. Appl. Geochem. 26, 1777–1791. https://doi.org/10.1016/j.apgeochem.2011.06.002.
Pohle, I., Baggaley, N., Palarea-Albaladejo, J., Stutter, M., Glendell, M., 2021. A Framework for Assessing Concentration-Discharge Catchment Behavior From Low-Frequency Water Quality Data. Water. Resour. Res. 57 (9) https://doi.org/10.1029/2021WR029692.
Reddy, K.R., Kadlec, R.H., Flaig, E., Gale, P.M., 1999. Phosphorus retention in streams and wetlands: A review. Crit. Rev. Environ. Sci. Technol. 29 (1), 83–146. https://doi.org/10.1080/10643389991259182.
Root, R.A., Hayes, S.M., Hammond, C.M., Maier, R.M., Chorover, J., 2015. Toxic metal (loid) speciation during weathering of iron sulfide mine tailings under semi-arid climate. Appl. Geochem.: J. Int. Assoc. Geochem. Cosmochem. 62, 131–149. https://doi.org/10.1016/j.apgeochem.2015.01.005.
Rose, L.A., Karwan, D.L., Godsey, S.E., 2018. Concentration–discharge relationships describe solute and sediment mobilization, reaction, and transport at event and longer timescales. Hydrol. Process. 32, 2829–2844. https://doi.org/10.1002/hyp.13235.
Sanchez, A.A., Mladenov, N., Wasswa, J., 2020. Fluorescent compounds retained by ultrafiltration membranes for water Reuse. J. Membr. Sci. 600, 117867 https://doi.org/10.1016/j.memsci.2020.117867.
She, Z., Wang, J., He, C., Jiang, Z., Pan, X., Wang, M., Ma, D., Shi, Q., Yue, Z., 2023. Molecular insights into the impacts of acid mine drainage on dissolved organic matter dynamics in pit lakes. Sci. Total Environ. 888 https://doi.org/10.1016/j.scitotenv.2023.164097.
Skousen, J.G., Ziemkiewicz, P.F., McDonald, L.M., 2019. Acid mine drainage formation, control and treatment: Approaches and strategies. Extr. Indus. Soc. 6, 241–249.
Tao, Y., Shen, L., Feng, C., Yang, R., Qu, J., Ju, H., Zhang, Y., 2022. Distribution of rare earth elements (REEs) and their roles in plant growth: A review. Environ. Pollut. 298, 118540 https://doi.org/10.1016/j.envpol.2021.118540.
Tiwary, R.K., 2001. Environmental impact of coal mining on water regime and its management. Water. Air. Soil. Pollut. 132, 185–199. https://doi.org/10.1023/A:1012083519667.
Tiwary, R.K., Dhar, B.B., 1994. Environmental pollution from coal mining activities in Damodar river basin, India. Mine Water. Environ. 13 (1), 1–10.
Wang, H., Li, Z., Zhuang, W.E., Hur, J., Yang, L., Wang, Y., 2020. Spectral and isotopic characteristics of particulate organic matter in a subtropical estuary under the influences of human disturbance. J. Marine Syst. 203 https://doi.org/10.1016/j.jmarsys.2019.103264.
Wang, Y., Tian, X., Song, T., Jiang, Z., Zhang, G., He, C., Li, P., 2023. Linking DOM characteristics to microbial community: The potential role of DOM mineralization for arsenic release in shallow groundwater. J. Hazard. Mater. 454 https://doi.org/10.1016/j.jhazmat.2023.131566.
Wasswa, J, Mladenov, N, Pearce, W., 2019. Assessing the potential of fluorescence spectroscopy to monitor contaminants in source waters and water reuse systems. Environ. Sci.: Water Res. Technol. 5, 370–382.
Watari, T., Nansai, K., Nakajima, K., 2021. Major metals demand, supply, and environmental impacts to 2100: A critical review. Resour. Conserv. Recycl. 164, 105107.
Weishaar, J.L., Aiken, G.R., Bergamaschi, B.A., Fram, M.S., Fujii, R., Mopper, K., 2003. Evaluation of specific ultraviolet absorbance as an indicator of the chemical composition and reactivity of dissolved organic carbon. Environ. Sci. Technol. 37 (20), 4702–4708. https://doi.org/10.1021/es030360x.
Wickham, H., 2016. ggplot2: Elegant Graphics for Data Analysis. Springer-Verlag, New York. https://ggplot2.tidyverse.org.
Wolkersdorfer, C., Walter, S., Mugova, E., 2022. Perceptions on mine water and mine flooding – An example from abandoned West German hard coal mining regions. Resour. Policy. 79 https://doi.org/10.1016/j.resourpol.2022.103035.
Yamashita, Y., Tanoue, E., 2003. Chemical characterization of protein-like fluorophores in DOM in relation to aromatic amino acids. Mar. Chem. 82, 255–271. https://doi.org/10.1016/s0304-4203(03)00073-2.
Zhang, K., Gao, J., Men, D., Zhao, X., Wu, S., 2021. Insight into the heavy metal binding properties of dissolved organic matter in mine water affected by water-rock

interaction of coal seam goaf. Chemosphere 265. https://doi.org/10.1016/j.chemosphere.2020.129134.
Zhiteneva, V., Brune, J., Mischo, H., Weyer, J., Simon, A., 2016. Water Quality of Reiche Zeche mine, Freiberg/Saxony, Germany. SME Ann. Meeting Conf.
Zhu, K., Hopwood, M.J., Groenenberg, J.E., Engel, A., Achterberg, E.P., Gledhill, M., 2021. Influence of pH and dissolved organic matter on iron speciation and apparent iron solubility in the peruvian shelf and slope region. Environ. Sci. Technol. 55 (13), 9372–9383. https://doi.org/10.1021/acs.est.1c02477.